

Biogenic composition of calcium carbonate over the past 140,000 years: clues from a marine core in the Santos Basin

Mariana Oliva Tomazella^{1,*}, Guilherme Augusto Pedrão¹, Juliana Pereira Quadros²,
Felipe Antonio de Lima Toledo¹, Karen Badaraco Costa¹

¹ Instituto Oceanográfico – Universidade de São Paulo (Praça do Oceanográfico, 191 - Cidade Universitária - Butantã - 05508-120 - SP – Brazil)

² Centro de Formação em Ciências Ambientais – Universidade Federal do Sul da Bahia (Rodovia BR-367 Km 10, S/n - Zona Rural - 45810000 - Porto Seguro - BA - Brazil)

* Corresponding author: mariana.tomazella@usp.br

ABSTRACT

This study aimed to investigate the biogenic composition of calcium carbonate (CaCO_3) in pelagic sediments in the Santos Basin over the past 140,000 years. The content and composition of CaCO_3 in different sediment fractions were evaluated, including the bulk sample, coarse fraction (foraminifera), medium fraction (juvenile foraminifera and fragments), and fine fraction (nanofossils), to determine the contribution of each fraction to the carbonated sediment composition. We found that variations in CaCO_3 levels were closely linked to glacial and interglacial periods, with higher values during interglacial periods and lower values during glacial periods. The main factor controlling the variation in CaCO_3 was dissolution, which was mainly linked to the influx of more corrosive southern water masses. Fluctuations in CaCO_3 levels were influenced by variations in productivity and dilution caused by terrigenous sediments. Nevertheless, it is noteworthy that both processes held a relatively minor impact compared to dissolution. Productivity primarily contributed to increased dissolution rates. During periods of low sea levels, dilution by terrigenous sediments became significant (similarly, the influence of the La Plata River plume was notable). However, due to the limited presence of riverine supply in the study area, which contributes directly to major dilution influences, fluctuations in terrigenous materials were considered of lesser magnitude than those caused by dissolution. The nanofossils were found to be the largest contributor to the total CaCO_3 composition, as they were the fraction least affected by the dissolution process. Overall, our results provide insights into the factors influencing CaCO_3 accumulation in marine sediments and can be used as a tool to determine changes between climatic cycles over time.

Keywords: Glacial-Interglacial Cycles, South Atlantic, Paleoceanography, Dissolution, Microfossils, Geochemistry

INTRODUCTION

The ocean plays a crucial role as a carbon reservoir, with most of the carbon being a vital

component of the calcium carbonate (CaCO_3) cycle. This cycle influences the pH of seawater and regulates the CO_2 exchange between the ocean and the atmosphere, making it an essential factor in climate change (Millero, 1996).

The primary mechanisms by which CO_2 is removed from the atmosphere are the biological pump and the storage of CaCO_3 in marine sediments and coral reefs (Volk and Hoffert, 1985; Charles

Submitted: 26-Apr-2023

Approved: 06-Dec-2023

Editor: Rubens Lopes



© 2024 The authors. This is an open access article distributed under the terms of the Creative Commons license.

and Fairbanks, 1990; Falkowski, 1997; Ducklow et al., 2001; Chiu and Broecker, 2008). Climate change significantly affects these processes, particularly during the transitions between glacial and interglacial periods (Volk and Hoffert, 1985; Broecker and Peng, 1986; Broecker, 2009). Marine organisms that produce CaCO_3 use dissolved inorganic carbon and calcium to create their shells. As a result, there is a reduction in the concentration of CO_3^{2-} in seawater, leading to an increase in the concentration of aqueous CO_2 and, ultimately, an increase in atmospheric CO_2 (Broecker, 2003; Chiu and Broecker, 2008). Conversely, a decrease in the CaCO_3 stock during glacial periods reduces CO_2 in the atmosphere. Therefore, carbonate deposition plays a vital role in regulating the climate by “sequestering” CO_2 (Millero, 1996; Bachu, 2000; Feely et al., 2004; Chiu and Broecker, 2008; Hassenkam et al., 2011).

Deep marine sediments consist primarily of CaCO_3 and clay minerals. In these areas, planktonic organisms such as nannofossils and foraminifera are the main producers of CaCO_3 (Frenz et al., 2005), whereas clay minerals originate from continental regions (Kullenberg, 1953; Broecker et al., 1958; Milliman, 1993; Balch et al., 2000). In terms of quantity, the main organisms that produce CaCO_3 are nannofossils, which are unicellular algae that secrete calcareous plaques known as coccoliths (Westbroek et al., 1993).

Foraminifera contributes more to carbonate production in mesotrophic regions, whereas nannofossils are more prevalent in oligotrophic regions. The relationship between the carbonate produced by these two organisms can indicate whether carbonate production serves as a source or sink for CO_2 (Buitenhuis et al., 1996; Frenz et al., 2005).

The amount of CaCO_3 present in deep marine sediments is influenced by four main factors: surface biological productivity, dilution by noncarbonate materials, diagenetic alterations, and dissolution. It may seem logical that an increase in productivity would lead to greater accumulation and preservation of CaCO_3 ; however, this is not always the case (Volat et al., 1980). An increase in productivity can: (a) boost the flow of organic carbon, which can lead to increased dissolution of CaCO_3 due to organic matter oxidation (Farrel and Prell, 1989) and (b)

support siliceous organisms, leading to dilution (Dymond and Collier, 1988).

The amount of CaCO_3 in sediments can also be diluted by an increase in the sedimentation of other materials, such as terrigenous material. Researchers such as Schott (1935) argue that during glacial periods in the Atlantic Ocean, there is an increase in the rate of carbonate accumulation, which is obscured by a simultaneous increase in the rate of noncarbonate materials (Hays and Peruzza, 1972; Arz et al., 2001; Baumann et al., 2004).

From tropical to temperate regions, at depths above the calcite compensation depth (CCD), the coarse fraction ($> 63 \mu\text{m}$) of pelagic sediments is primarily composed of foraminifera. Juvenile foraminiferal tests and fragments dominate the medium fraction ($63\text{--}20 \mu\text{m}$), whereas the fine fraction ($< 20 \mu\text{m}$) is dominated by nannofossils (Broecker and Clark, 1999; Ziveri et al., 2000; Broecker and Clark, 2001; Frenz et al., 2005; Ramaswamy and Gaye, 2006; Chiu and Broecker, 2008). Additionally, the division of the carbonate content into different size fractions has been used as a supplementary method for determining the effects of dissolution based on an index proposed by Chiu and Broecker (2008). Broecker and Clark (1999) also propose that the relationship between the contributions of different size fractions of CaCO_3 in the composition of total CaCO_3 can be used as a proxy to determine the composition of marine CaCO_3 , which is related to climate change.

Broecker and Clark (1999) analyzed the CaCO_3 content in the top core samples for the bulk sediment and one sediment fraction ($> 63 \mu\text{m}$) and found that the ratio between them decreased linearly with depth. They also discovered that the contribution of nannofossils was greater in glacial periods than in interglacial periods when analyzing samples from both (Broecker and Clark, 2001). Therefore, analysis of carbonate biogenic composition can be used as a tool to better understand regional and global climate oscillations.

This study aimed to evaluate the CaCO_3 content/composition in pelagic sediments and to estimate the contribution of each fraction to the carbonated sediment composition. Additionally, another aim was to verify whether this contribution has changed over the last 140,000 years in the

western portion of the South Atlantic (Santos Basin) and the possible causes of this variation.

METHODS

STUDY AREA

The Santos Basin, in southeastern Brazil, holds a limited amount of terrigenous input due to the uplift of the Serra do Mar, which causes most of the drainage basins in the region to flow inland instead of directly into the ocean. Therefore, sedimentation and sediment redistribution in the area are primarily controlled by factors such as ocean currents and water masses, primary productivity, sea level changes, and the climate of the surrounding land (Stein, 1991; De Mahiques et al., 2004).

De Mahiques et al. (2004) divided the southern region of the Brazilian coast into two sedimentation zones. The depositional processes in the northern zone are controlled by the meanderings of the Brazil Current (BC), whereas in the southern zone, seasonal penetration of a low-salinity and low-temperature plume from the Rio de la Plata River estuary influences the depositional processes (De Mahiques et al., 2009, Gyllencreutz et al., 2010, Mathias et al., 2014). This plume extends to latitude 32°S in spring and 28°S in winter and can lead to higher productivity when it interacts with

the BC, as it is also an important nutrient source for the ocean (Piola et al., 2000). Additionally, under favorable wind conditions, the plume can reach as far north as 23°S (Campos et al., 1999).

The surface circulation of the South Atlantic Ocean is controlled by an anticyclonic gyre, which dominates the upper 1,000 meters of depth. The BC presence flowing southward also affects the local hydrodynamics. The BC emerges from the bifurcation of the southern portion of the South Equatorial Current, transporting Tropical Water (TW), which is hot, saline, and low in nutrient concentrations (Emilson, 1961; Peterson and Stramma, 1991; Campos et al., 1995; Ciotti et al., 1995; Silveira et al., 2000; Cirano et al., 2006). The BC is 500 meters deep and 100 kilometers wide and can create meanders and eddies on the continental shelf and slope (Campos et al., 1995; 1999).

The water masses present in the study area include the South Atlantic Central Water (SACW), Antarctic Intermediate Water (AAIW), Upper Circumpolar Water (UCPW), North Atlantic Deep Water (NADW), Lower Circumpolar Water (LCPW), and Antarctic Bottom Water (AABW) (Peterson and Stramma, 1991; Silveira et al., 2000). The core collection depth of 2,225 m is under the influence of the NADW and is located near a mixing zone between the NADW and the UCPW (Figure 1).

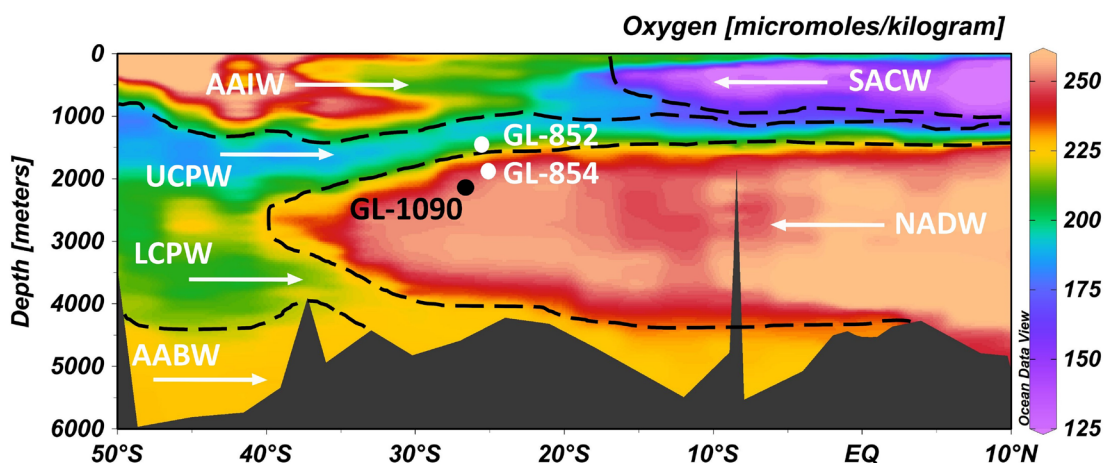


Figure 1. Schematic representation of the South Atlantic Ocean water masses based on GEOSECS v2 dissolved oxygen data (Bainbridge and GEOSECS, 1981). Black dot represents the GL-1090 position under the influence of the North Atlantic Deep Water (NADW). White dots represents other records discussed in this work, GL-852 and GL-854 (Lessa et al., 2019). Dashed black lines represent water masses limits. White arrows represent the flow directions of the respective water masses: AAIW- Antarctic Intermediate Water, SACW – South Atlantic Central Water, UCPW – Upper Circumpolar Water, NADW – North Atlantic Deep Water, LCPW – Lower Circumpolar Water, and AABW - Antarctic Bottom Water.

The NADW is found at depths of 1,500m to 3,000m off the coast of Southeast Brazil (Peterson and Stramma, 1991; Silveira et al. 2000). It is noncorrosive to CaCO_3 (Arz et al., 1999) and holds low concentrations of CO_2 and nutrients (Dittert et al., 1999). The division of the Antarctic Circumpolar Water (ACPW) by the NADW forms two different sections (upper and lower). Compared to the NADW, the upper section (UCPW) is less saline, low in oxygen, and high

in phosphate and causes a corrosive effect on CaCO_3 due to its high concentration of CO_2 (Dittert et al., 1999).

MATERIALS

This study was based on the analysis of a core, GL-1090, located at $25^\circ 11' \text{ S}$ and $44^\circ 43' \text{ W}$, at a water depth of 2,225 m on the continental slope of the Santos Basin in the western South Atlantic (Figure 2).

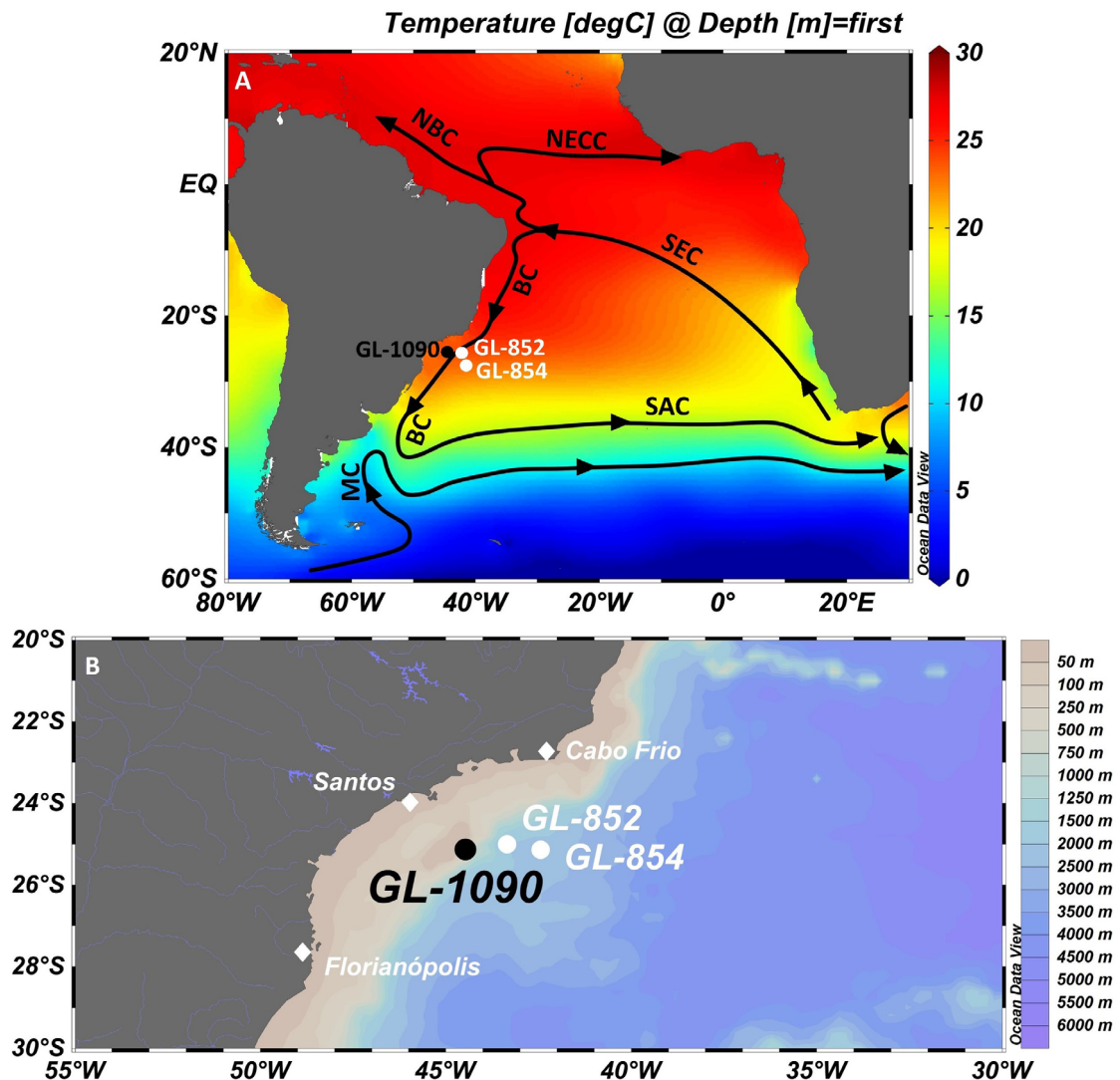


Figure 2. Overview of the South Atlantic surface circulation and Santos Basin. **(A)** Depiction of the sea surface temperature distribution and GL-1090 study site, modified from Peterson and Stramma (1991). BC: Brazil Current, MC: Malvinas Current, NBC: North Brazil Current, SAC: South Atlantic Current, SEC: South Equatorial Current, and NECC: North Equatorial Counter Current. **(B)** Geographical representation of the Santos Basin with river systems and isobath depths. White dots represents other records discussed in this work, GL-852 and GL-854 (Lessa et al., 2019).

The sediment core GL-1090 was collected using a piston corer with a total recovery of 1,914 cm. To conduct this research, a total of 57 representative samples were selected from the 438 available, encompassing different paleoceanographic/climatic conditions (glacial, deglacial, and interglacial).

STABLE ISOTOPES AND AGE MODEL

In the study conducted by Santos et al. (2017), isotopic analyses were performed on benthic and planktonic foraminifera using approximately ten shells of each species within the 250–300 μm size range. For the benthic analysis, the chosen species was *Cibicides wuellerstorfi*. In cases where an insufficient quantity of *C. wuellerstorfi* samples was available, the alternative species *Uvigerina peregrina* was selected. The $\delta^{18}\text{O}$ and $\delta^{13}\text{C}$ values were accurately determined, and additional details can be found in Santos et al. (2017). Planktonic foraminifera analyses focused specifically on the white variety (*sensu stricto*) of *Globigerinoides ruber*.

The experimental procedures were conducted at the MARUM – Center for Marine Environmental Sciences, University of Bremen, Germany. A Finnigan MAT251 gas isotope ratio mass spectrometer was used in conjunction with a Kiel III automated carbonate preparation device. The standard deviations, calculated based on multiple measurements of the internally employed standard, were established at 0.06‰ for $\delta^{18}\text{O}$ and 0.04‰ for $\delta^{13}\text{C}$.

The chronology was determined by Santos et al. (2017, 2020) by correlating the $\delta^{18}\text{O}$ data in benthic foraminifera with two reference curves: LR04 (Lisiecki and Raymo, 2005) and MD95-2042, as modified by Govin et al. (2014), using the most recent ice core chronology AICC2012 (Veres et al., 2013). The complete age model was then built using Bacon v. 2.3 software, which employs Bayesian statistics to reconstruct the accumulation rates of downcore age-depth relations (Blaauw and

Christen, 2011). Bacon was employed with default parameters, applying 10,000 age-depth runs to estimate the mean age and 95% confidence interval at the desired resolution for each proxy, as described in more detail in Santos et al. (2020).

Six marine isotopic stages (MIS) can be recognized in the record for the last 140,000 years, comprising the last glacial–interglacial cycle. MIS 1 and 5 represent interglacial periods, whereas stages 2–3–4 and 6 represent glacial periods.

VARIATION IN CaCO_3 IN THE DIFFERENT FRACTIONS

The samples for analysis were prepared at the South Atlantic Paleooceanography Laboratory (LaPAS-IOUSP) following a systematic procedure. First, a portion of the bulk sample was isolated to determine the total CaCO_3 content. Then, the remaining sample was weighed and subjected to wet sieving using two different mesh sizes: 63 μm and 20 μm . This process resulted in three distinct fractions: < 20 μm (fine), 20–63 μm (medium), and > 63 μm (coarse).

After wet sieving, the fractions were dried in an oven at 50 °C and then reweighed (Weight 1). Next, to remove the CaCO_3 , the samples were treated with 10% hydrochloric acid (HCl). Any excess acid was carefully removed, and the samples were thoroughly washed with water to eliminate any traces of remaining acid. Finally, the samples were dried again and weighed to determine their weight without CaCO_3 (Weight 2).

Notably, the coarse fraction was not used in the acidification process. This decision was made because the method employed for analysis is destructive, and this fraction needs to be preserved for planktonic foraminiferal assemblage analyses.

To calculate the amount of CaCO_3 in each fraction, the initial weight (Weight 1) and final weight (Weight 2) of each subsample were used (Equation 1).

Additionally, the percentage of CaCO_3 in each fraction was calculated (Equation 2).

$$(\text{Weight 2} - \text{Weight 1}) = \text{Weight in grams of calcium carbonate} \quad (1)$$

$$\text{Weight in grams of calcium carbonate} \times 100 / \text{Weight 1} \quad (2)$$

To assess the representative percentage of each fraction in the total CaCO_3 composition (Equation 3)

of the sample, the weight of each fraction in grams of CaCO_3 was compared to the total weight of CaCO_3 .

$$\text{Weight in grams of calcium carbonate} \times 100 / \text{Total weight of CaCO}_3 \text{ in the sample} \quad (3)$$

As we did not measure the carbonate content of the coarse fraction, we determined its contribution

by subtracting the contribution (in percentage) of the other fractions (Equation 4).

$$\text{Coarse fraction} = (100 - (\text{fine fraction} + \text{medium fraction})) \quad (4)$$

DISSOLUTION INDEX

The variation in CaCO_3 content in different size fractions was also used to establish the dissolution index, as proposed by Chiu

and Broecker (2008), using the following equation: (Equation 5).

A higher value of the index indicates a greater influence on dissolution processes.

$$\frac{\% \text{CaCO}_{3 < 20 \mu\text{m}}}{(\% \text{CaCO}_{3 > 20 \mu\text{m}} + \% \text{CaCO}_{3 < 20 \mu\text{m}})} \quad (5)$$

RESULTS

SEDIMENTOLOGY

The sedimentation in the GL-1090 core was continuous, and the core was predominantly composed of intercalations of marls and mudstones. The coarse fraction was mainly

composed of planktonic foraminifera. To better understand its composition, the sediments were classified based on their CaCO_3 content. Marls (M) were characterized by a CaCO_3 content of 30–60%, carbonate-rich mud (CR) held a CaCO_3 content of 18–30%, and light carbonate mud (LC) held a CaCO_3 content of 5–18% (Figure 3).

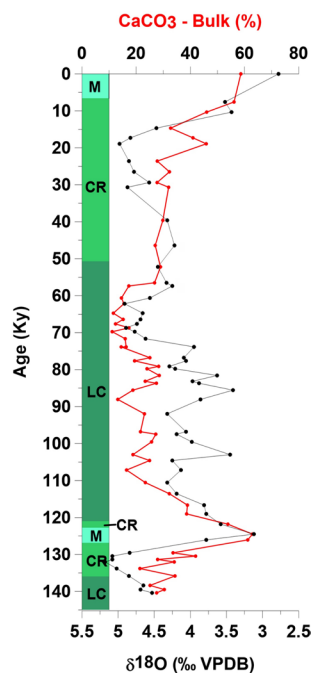


Figure 3. Lithology and geochemical variations in the GL-1090 Core. The green bars represent the GL-1090 lithology. The red line represents the CaCO_3 content, and the black line shows the benthic $\delta^{18}\text{O}$ variations over time. M represents Marl, CR represents Carbonate-rich Mud, and LC represents Light Carbonate Mud.

ISOTOPIC STRATIGRAPHY

The oxygen isotope records measured in benthic foraminifera plotted as a function of age (Figure 4) revealed features that correlate with the LR-04 stack (Lisiecki and Raymo, 2005). Six marine isotopic stages (MIS) can be recognized in the record of the last 140,000 years, comprising the last glacial–interglacial cycle. MIS 1 and 5 represent interglacial periods, whereas stages 2–3–4 and 6 represent glacial periods

(Figure 4). The marine isotopic stages were determined according to the time limits established by Lisiecki and Raymo (2005).

MIS 6 showed the highest values of benthic $\delta^{18}\text{O}$. MIS 5 held the second lowest value of benthic $\delta^{18}\text{O}$, representing the last interglacial period. This core's 4–3 and 3–2 boundaries were unclear. MIS 2 showed high values of benthic $\delta^{18}\text{O}$, representing the Last Glacial Maximum (LGM). Finally, stage 1, an interglacial interval equivalent to the Holocene, showed the lowest values of benthic $\delta^{18}\text{O}$ (Figure 4).

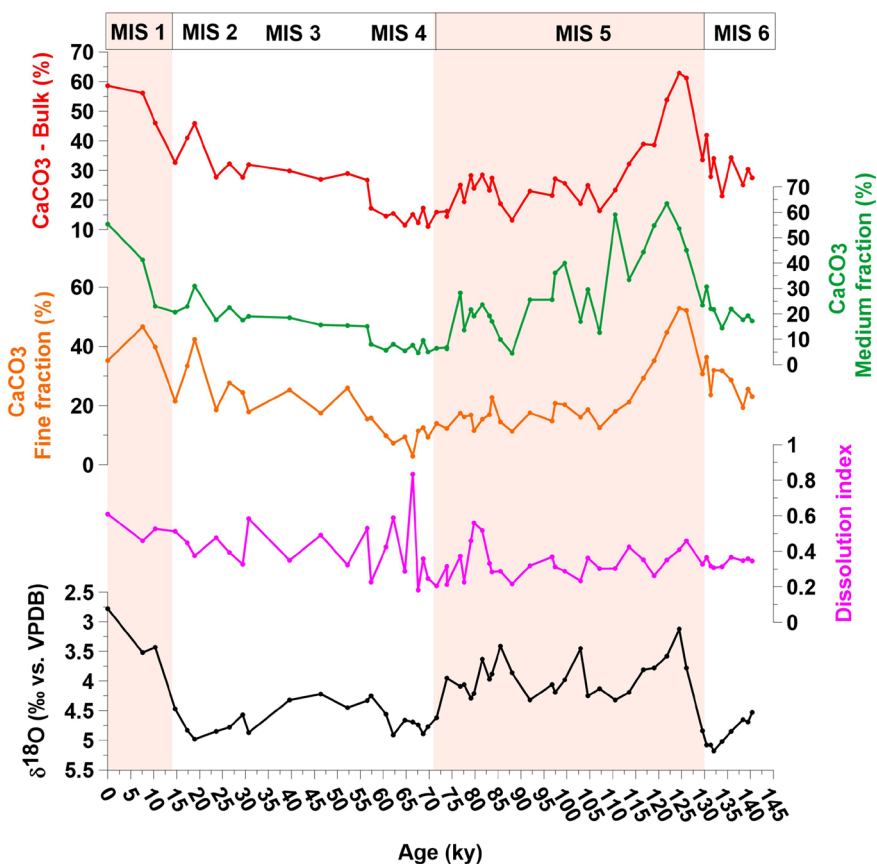


Figure 4. Illustration of the relationship between benthic $\delta^{18}\text{O}$ values (in black) and age in the GL-1090 Core. The time periods from MIS 6 to 1 are indicated as defined by Lisiecki and Raymo (2005). Interglacial periods are highlighted with red bars. Three different fractions of CaCO_3 content (measured in the fraction itself) are shown: Bulk (in red), Medium-Fraction (in green), and Fine-Fraction (in orange). These lines demonstrate the changing connections between CaCO_3 content in various size fractions and benthic $\delta^{18}\text{O}$ values. The Dissolution Index (in pink) is calculated by assessing the $<20\ \mu\text{m}$ and $>20\ \mu\text{m}$ CaCO_3 sediment fractions within the GL-1090 core. This calculation, developed by Chiu and Broecker (2008), is used for evaluating carbonate preservation.

CaCO_3 CONTENT IN THE DIFFERENT FRACTIONS

The percentages of CaCO_3 in the bulk, medium (20 to 63 μm), and fine ($< 20\ \mu\text{m}$) fractions were

similar, with their fluctuations following the benthic $\delta^{18}\text{O}$ curve, that is, lower values of CaCO_3 content during glacial periods and higher values during

interglacial periods. The results obtained for each fraction are presented in detail below ([Table S1, Supplementary Material](#)).

TOTAL CALCIUM CARBONATE

The percentage of total CaCO_3 in the bulk fraction fluctuated from 10% to 60%, following the pattern of the benthic $\delta^{18}\text{O}$ curve, with higher percentages during interglacial periods and lower percentages during glacial periods (Figure 4). The highest percentage of CaCO_3 was observed in the Last Interglacial (MIS 5e), and the lowest percentage was approximately 65,000 years ago during the MIS 4 glacial stage.

MEDIUM FRACTION CARBONATE

In the medium fraction (20 to 63 μm), CaCO_3 percentages fluctuated from 10 to 70%, with its highest values observed in the Last Interglacial

(MIS 5e) and its lowest values in the MIS 4 glacial stage (Figure 4). The percentages then increased again to approximately 55% in the Holocene. This fraction held the highest percentages of CaCO_3 , reaching up to 70%.

FINE FRACTION CARBONATE

The fine fraction showed the lowest percentage of carbonate. It varied from approximately 5 to 55%, with its highest values in the Last Interglacial (MIS 5e) and lowest values in MIS 4. High values (~45%) reappeared in the Holocene (Figure 4).

CONTRIBUTION OF EACH FRACTION TO TOTAL CaCO_3

In general, the fine fraction showed the highest percentage of contribution to total carbonate, followed by the coarse fraction (> 63 μm) and the medium fraction, which held the lowest contribution (Figure 5).

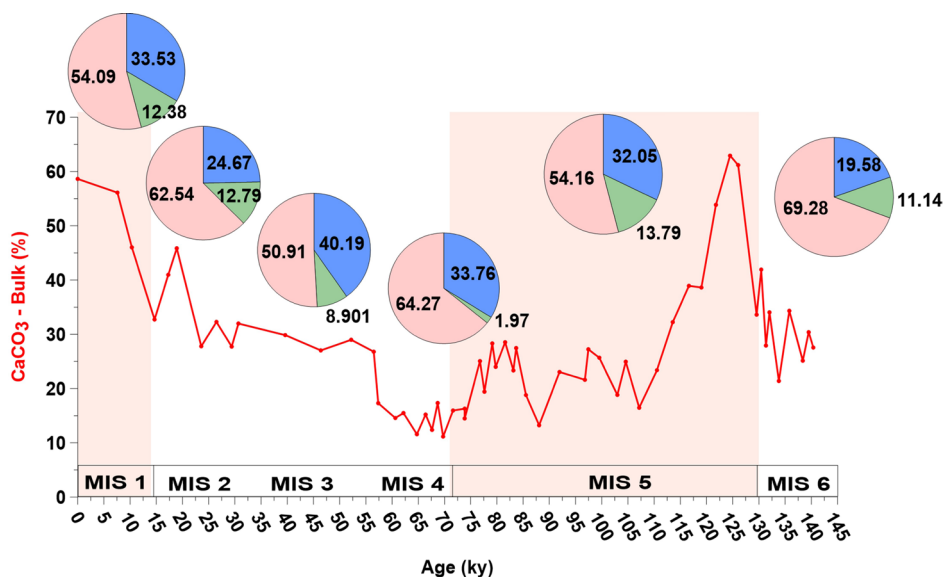


Figure 5. Variation of sediment fractions contribution to total CaCO_3 composition in the GL-1090 core. This figure presents the percentage contribution of coarse (blue), medium (green), and fine (pink) sediment fractions to the total CaCO_3 , as represented by pie charts for each sample characteristic of a Marine Isotopic Stage (MIS). The red line represents the bulk fraction CaCO_3 percentage (measured in the fraction itself).

The most prominent variations in the contributions of the different fractions were observed during the glacial and interglacial periods (Figure 5). During the glacial periods, the fine fraction showed a greater contribution compared to the other fractions, whereas during the interglacial periods, the fine fraction

continued to be the main contributor to the CaCO_3 content, but with a decrease in its contribution. In the same period, we observed an increase in the contribution of the coarse fraction. The medium fraction contribution remained relatively constant throughout all the isotopic stages, except in MIS 4, where there

was a significant reduction in its proportion, which was almost non-existent.

The contribution of the coarse fraction varied from 20 to 60% of the total CaCO_3 content (Figure 6). From 140 to 90 ky, there was a variation of approximately 20–40% and, after this period, there was an increase until the top of the core, with values ranging from 20 to 60%.

The medium fraction showed the smallest variation, from 2 to 18%, and contributed the

least to the composition of total CaCO_3 content (Figure 6). The maximum value was observed in MIS 6, approximately 135 ky, and the minimum was observed at 72 ky, near the boundary of MIS 5/4. The contribution of this fraction reaches higher values from 140 to 130 ky, with a subsequent decrease to minimum values of ~72 ky. Subsequently, the values increased again, maintaining a positive trend until the top of the core.

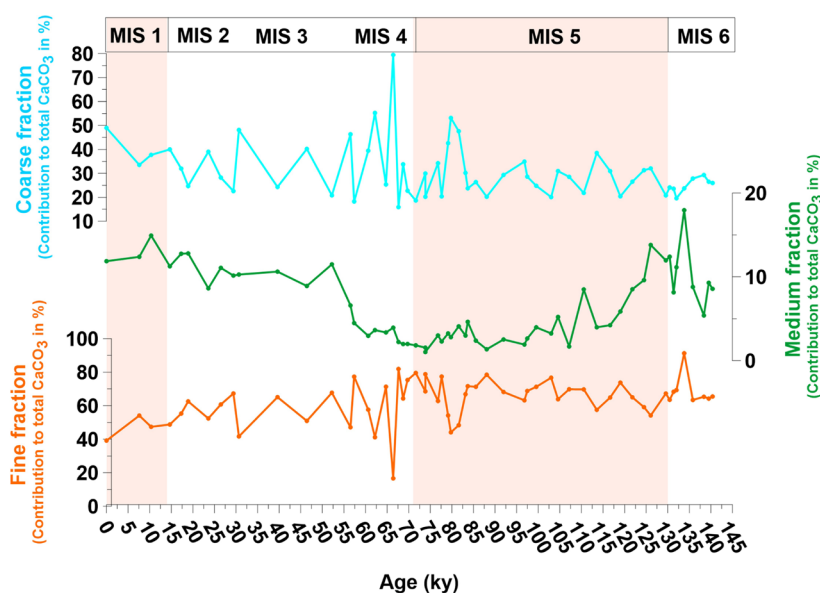


Figure 6. Evolution of the sediment fractions' contribution to total CaCO_3 in the GL-1090 core. This figure displays the proportion of coarse, medium, and fine sediment fractions to the total CaCO_3 composition across different Marine Isotopic Stages (MIS 6 to 1) marked on the figure.

The fine fraction contributed the most to the CaCO_3 composition and showed the greatest variation in contribution, with values ranging from 40 to 90%. The minimum contribution (40%) was established in MIS 2, and the maximum (90%) was at 135 ky in MIS 6. The data show an increasing trend in the contribution from 130 to 65 ky. From the age of 65 ky, this trend reversed and started to decrease until the top of the core (Figure 6).

DISSOLUTION INDEX

The dissolution index proposed by Chiu and Broecker (2008) is a measure of the degree of dissolution of the sediment. Data analysis of the

GL-1090 core revealed an increase in dissolution rates at the end of the Last Interglacial (MIS 5, approximately 80 ky), at the beginning of the MIS 4 glacial period, and throughout the MIS 4, 3, and 2 glacial stages (Figure 4). In other periods, such as MIS 1 and most of MIS 5, the index indicated good preservation.

DISCUSSION

CaCO_3 CONTENTS

The variation in CaCO_3 content was consistent across all analyzed fractions. An increase in CaCO_3 content was observed during interglacial periods and a decrease during glacial periods, which is a common pattern in Atlantic Ocean marine sediment

cores (Olausson, 1965, 1971; Gardner, 1975; Thunell, 1976). However, this pattern is opposite to that observed in Pacific Ocean sediment cores, as demonstrated by Berger (1973) and Thompson and Saito (1974). Factors that can affect the distribution of CaCO_3 during glacial and interglacial periods include productivity, dilution by noncarbonate materials, and dissolution (Arz et al., 1998; Govin et al., 2014).

PRODUCTIVITY

Several authors have reported an increase in paleoproductivity during glacial periods (MIS 6, 4, and 2) and a decrease during interglacial periods for the South Atlantic Ocean (MIS 5 and 1) (Schmiedl and Mackensen, 1997; Chiu and Broecker, 2008; Nagai et al., 2010; Pereira et al., 2018; Portilho-Ramos et al., 2019; Pedrão et al., 2022; Suárez-Ibarra et al., 2022).

One method to estimate the variation in productivity rate is by measuring the difference between the carbon isotope ratio between benthic and planktonic foraminifera ($\Delta\delta^{13}\text{C}$). This difference is controlled by the production of organic matter by photosynthesis on the surface, which depletes ^{12}C stocks, and by the regeneration of organic matter at depth, which makes inorganic ^{12}C available again in deep waters. Therefore, a larger difference between planktonic and benthic ($\Delta\delta^{13}\text{C}$) indicates higher productivity (Broecker, 1982; Shackleton et al., 1983; Curry and Crowley, 1987). In this study, $\Delta\delta^{13}\text{C}$ showed similar productivity during glacial and interglacial periods (Figure 7). The *Globigerina bulloides* and *Globigerinoides ruber* ratio (Gb/Gr) calculated by Lessa et al. (2019) in the Santos Basin was also used to estimate the paleoproductivity parameter.

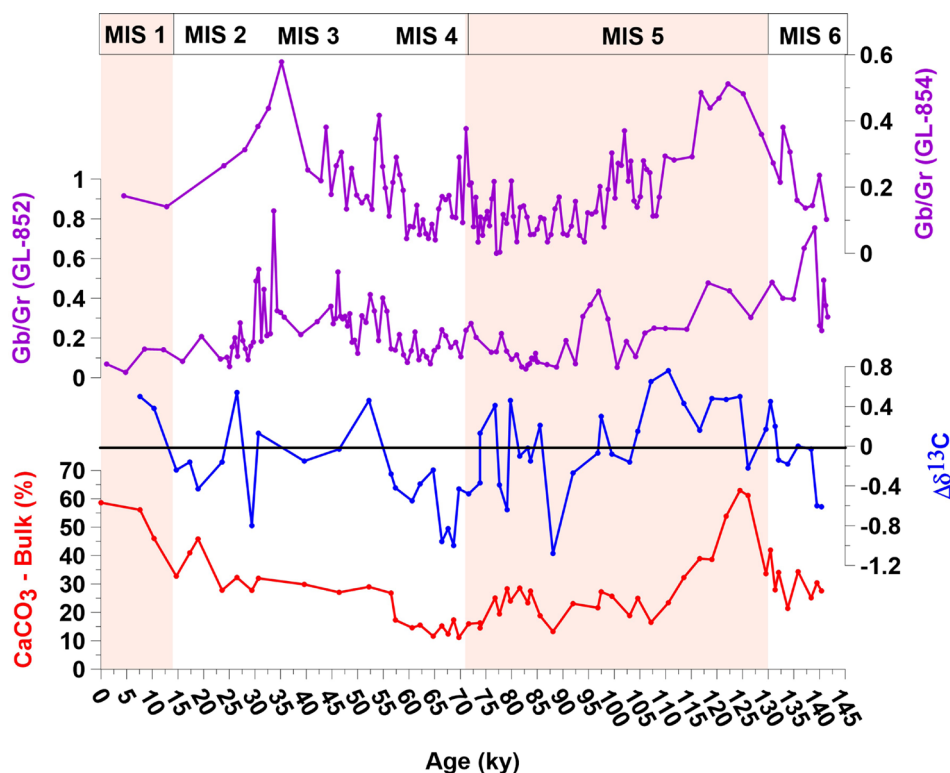


Figure 7. A visual representation showcases productivity assessments derived from the disparity in $\delta^{13}\text{C}$ values between benthic and planktonic foraminifera. These data are plotted in correlation with the bulk CaCO_3 content (measured within its respective fraction). A greater discrepancy in $\Delta\delta^{13}\text{C}$ values (depicted in blue) corresponds to a heightened level of productivity. Additionally, paleoproductivity estimates using the *G. bulloides* and *G. ruber* ratio (in purple) are presented on the graph. These estimates refer to the GL-852 and GL-854 cores within the same geographical region as the GL-1090 core. These calculations were carried out by Lessa et al. in 2019.

At first glance, productivity, as an enhancing factor, does not appear to be a controlling factor for CaCO_3 content in the area studied, as glacial periods showed the lowest CaCO_3 content and interglacial periods showed higher CaCO_3 rates, despite their similar productivity. According to Volat et al. (1980), variations in productivity do not necessarily lead to a variation in CaCO_3 levels. According to Dymond and Collier (1988), productivity may favor siliceous organisms, which will increase the effect of dilution by noncarbonate materials and increase the flow of organic carbon, which can lead to a more intense CaCO_3 dissolution due to the oxidation of organic matter. Therefore, productivity can act as a dissolution process.

The functioning of the oceanic carbonate pump system is significantly impacted by changes in bioproductivity. Increased biological surface productivity enhances respiration processes, leading to the release of CO_2 and reduced biological carbon burial. Additionally, the greater CO_2 release on the seafloor can cause increased dissolution of biogenic carbonates, as in planktonic foraminifera tests. Thus, an enhanced biological pump can unexpectedly reduce organic matter burial and dissolve biogenic carbonates, limiting the carbon storage in seafloor sediments. Notable studies by Cronin et al. (1999), Dittert et al. (1999), Schiebel (2002), Hales (2003), Zamelczyk et al. (2012) and Naik et al. (2014) have corroborated these findings.

Suárez-Ibarra et al. (2022) reconstructed data on productivity in the Pelotas Basin (South Atlantic) during glacial and interglacial periods and revealed variations in surface productivity, organic matter flux, and dissolution rates of planktonic foraminifera tests during glacial (high) and postglacial periods (low). The study also noted that an enhanced upwelling environment causes higher CO_2 concentrations and acidic conditions on the sea floor, resulting in varying levels of carbonate dissolution. With a multiple linear regression, the authors confirmed productivity as a controlling factor of CaCO_3 dissolution.

However, Gonzales et al. (2017) concluded that carbonate dissolution in the Santos Basin is not driven by organic matter oxidation (e.g., more productivity), since the Brazilian margin

is considered a low-latitude oligotrophic area, indicating low surface productivity (Rühlemann et al., 1999; Gaeta and Brandini, 2006; Brandini et al., 2018; Bordin et al., 2019). Paleooceanographic studies also suggest that this condition has likely persisted since the Last Glacial Maximum (LGM) (Toledo et al., 2007; Pivel et al., 2013).

DILUTION

The contribution of terrigenous material is considered a major factor in diluting the carbonate content in the studied area (Arz et al., 1998). By comparing the Fe/Ca (Figueiredo et al., 2020) data with the CaCO_3 data, we can observe an inverse relationship: an increase in the contribution of terrigenous sediments corresponds to a decrease in CaCO_3 levels and vice versa (Figure 8).

The increase in terrigenous input is primarily caused by the arrival of material by river input, which is linked to precipitation and sea level variations. In the Santos Basin, no river with significant fluvial discharge could directly affect marine sedimentation at present (De Mahiques et al., 2004).

Findings from analyzing major and minor elements in the GL-1090 core suggest that the composition of terrigenous sediments delivered to the research site was similar to the surface sediments currently deposited off the Plata River mouth (Mathias et al. 2021). Hence, the inference presented in this study is that the Plata plume served as an important source of terrigenous sediment during glacial maxima. Conversely, during interglacial sea-level high stands, a decrease in the northward transport of the Plata plume resulted in an overall reduction in terrigenous input to the study site.

Another factor controlling terrigenous sediment input is sea level variations (De Mahiques et al., 2009; Nagai et al., 2010; Govin et al., 2012; Mathias et al., 2014; Pedrão et al., 2021, 2022). A potential consequence of a decrease in sea level is the exposure of a larger portion of the continental shelf to erosion. Furthermore, during glacial periods, changes in glacial vegetation cover and precipitation patterns may contribute to increased erosion on the more exposed land, thereby intensifying the weathering process on the continent. This, in turn, can result in a higher input

of terrigenous sediments (Behling et al., 2000; Leite et al., 2016).

When reconstructing sea level variations over the period studied using data from Lea et al. (2002) (Figure 8), it was observed that sea level was

higher during interglacial periods and lower during glacial periods, which aligns with the terrigenous input data. Therefore, the dilution process clearly influences the CaCO_3 record in the study area, being primarily controlled by sea level fluctuations.

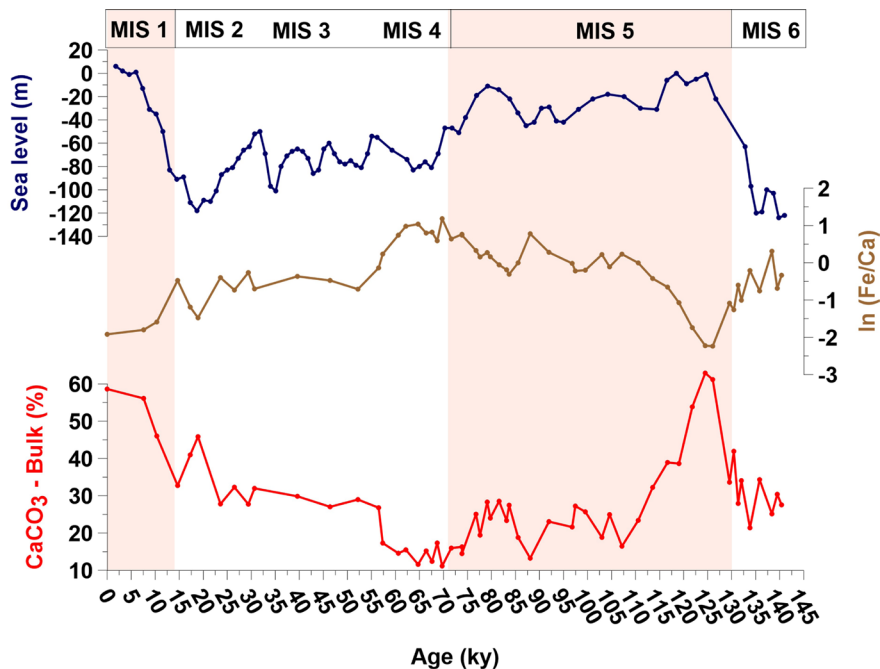


Figure 8. Plotting $\ln(\text{Fe}/\text{Ca})$ (in brown; Pedrão et al., 2021,2022) against bulk CaCO_3 data (in red) allows us to explore the correlation between the deposition of carbonate and noncarbonate materials, as well as the presence of CaCO_3 dilution. Additionally, the graph portrays the association between fluctuations in global sea levels (in deep blue) (as per Lea et al. 2002) and the influx of terrigenous sediment, as indicated by the $\ln(\text{Fe}/\text{Ca})$ values. This visual representation effectively underscores how changes in sea levels impact the introduction of terrigenous sediment into the investigated area.

DISSOLUTION

During glacial periods, dissolution processes are stronger than during interglacial periods, resulting in lower CaCO_3 preservation. The minimum levels of CaCO_3 content during glacial periods are correlated with dissolution events, such as those observed in MIS 4 and 6 (Crowley, 1983). The dissolution event in MIS 4 is more significant than that in MIS 6, as indicated by Chiu and Broecker's (2008) dissolution index calculated for GL-1090 (Figure 4). Additionally, Crowley (1983) suggests that the more significant dissolution event in MIS 4 is also reflected in the lower CaCO_3 values of this stage compared to those in MIS 2, which is the stage where the minimum temperature (maximum values of benthic $\delta^{18}\text{O}$) and, thus, where the minimum CaCO_3 content should theoretically occur.

The dynamics of the water masses in the study area play a role in the dissolution of CaCO_3 . During interglacial periods, the predominant water mass at the depth of GL-1090 is the NADW, which is less corrosive to CaCO_3 than the Antarctic Circumpolar Water (ACPW) flowing from the south. However, during glacial periods, the NADW becomes shallower and there is an intrusion of LCPW, which is more corrosive to CaCO_3 and thus increases dissolution and decreases preservation. This influence of southern water masses has previously been reported by several authors at depths of approximately 2,000 m in the South Atlantic (Clark et al., 2002; Rahmstorf, 2002; Curry and Oppo, 2005; Petró et al., 2018, 2021; Petró and Burone, 2018; Figueiredo et al., 2020).

NADW plays a crucial role in preserving carbonate, as it is oversaturated with carbonate

ions (CO_3^{2-}) compared to the overlying UCPW and the underlying LCPW and AABW. In contrast, UCPW, LCPW, and AABW are undersaturated in CO_3^{2-} , making them prone to carbonate dissolution (Frenz et al., 2004). The depth of the interface between the NADW and the AABW, as demonstrated by Frenz and Henrich (2006), represents the lysocline, which marks the level below which carbonate dissolution takes place.

The dissolution process affects all fractions, meaning that all fractions preserve less CaCO_3 during glacial periods and more CaCO_3 during interglacial periods. The difference lies in the proportion that each fraction preserves CaCO_3 during interglacial and glacial periods. The fine fraction tends to preserve more CaCO_3 during glacial periods compared to the other fractions, and the coarse fraction tends to preserve more CaCO_3 during interglacial periods compared to the other fractions.

The transfer of CaCO_3 among different fractions due to dissolution is well documented (Berger et al. 1982). The dissolution process breaks down larger fractions into smaller parts, creating a descending chain of CaCO_3 , which leads to an increase in the fine fraction and a decrease in the coarse fraction. Frenz and Henrich (2006) observed a relative decrease in the proportion of foraminifer carbonate and an increase in nannofossil carbonate, supporting the transfer of carbonate from coarser to finer grain-size fractions due to fragmentation and the assumption that foraminifers are more susceptible to carbonate dissolution than nannofossils.

Hay (1970) noted that nannofossils are more resistant to dissolution in deep waters than planktic foraminifera and other carbonate-secreting invertebrates. The transportation of nannofossils by fecal pellets is a crucial process in transferring small phytoplankton skeletons from the photic zone to the ocean floor, with the pellets acting as a protective shield. Additionally, the interstitial water of the fecal pellet shows a semi-independent nature from the surrounding deep-sea water, shielding them from the influence of adjacent water masses (Honjo, 1975, 1976; Honjo et al. 1982, Dittert et al., 1999).

Additionally, nannofossils hold a smaller amount of magnesian calcite in their carbonate structure,

which makes them less susceptible to dissolution (Bischoff et al., 1983). This variation in magnesium content between the structures of nannofossils and foraminifera can be observed by the Mg/Ca ratio of their shells, with nannofossils holding a significantly lower ratio than foraminifera. As a result, combined with the presence of pellets, nannofossils are less prone to dissolution compared to foraminifers (Pogge von Strandmann et al., 2014).

The medium fraction, however, tends to remain constant, as it is in the middle of the chain, losing some CaCO_3 to the fine fraction and gaining some from the coarse fraction. An unusual observation was made during MIS 4, where the medium fraction experienced a significant reduction in its contribution. This is likely due to the high dissolution rate observed during this period, as reported by Chiu and Broecker (2008). This observation supports the overall process described above.

CONCLUSION

The results of this study indicate that variations in CaCO_3 content over time are closely linked to glacial and interglacial periods. The balance between biogenic production of CaCO_3 in ion carbonate and carbon dioxide subsaturated surface waters and dissolution in supersaturated (ion carbonate and carbon dioxide) deep waters determines the distribution, preservation, and accumulation of CaCO_3 on the seafloor.

Productivity was investigated as a potential factor influencing CaCO_3 levels. Higher productivity rates during glacial periods were associated with lower CaCO_3 preservation. We concluded that productivity acts as a dissolution process, affecting the preservation of CaCO_3 more than its input to the ocean floor. Dilution by terrigenous materials, controlled by sea level fluctuations, emerged as another controlling factor, with higher terrigenous contributions associated with decreased CaCO_3 levels and vice versa; however, the terrigenous input into the region is limited by the low presence of riverine input.

The dissolution process has been identified as a key factor affecting CaCO_3 preservation, with stronger dissolution during glacial periods leading to lower CaCO_3 content. Dissolution events are mainly linked to the influx of more corrosive

water masses from the south, as proposed by Clark et al. (2002) and Rahmstorf (2002).

Among the main components of marine CaCO₃, nannofossils contributed the most to the total CaCO₃ composition, as they are the fraction (fine fraction) least affected by the dissolution process and the fraction that increases due to the effects of dissolution on the larger fractions. The CaCO₃ content of all the fractions varied similarly, making any one of the fractions suitable for analyzing the variation in CaCO₃ content in marine sediments. Additionally, CaCO₃ variations are similar to the benthic δ¹⁸O curve and can be used as a tool to determine changes between climatic, glacial, and interglacial cycles over time.

ACKNOWLEDGMENTS

The authors wish to express their gratitude to R. Kowsman (Centro de Pesquisas Leopoldo Américo Miguez de Mello, CENPES/Petrobras) and the Petrobras Core Repository staff (Macaé/Petrobras) for providing the sediment core used in this research. We are also grateful for funding from the Coordenação de Aperfeiçoamento de Pessoal de Nível Superior (CAPES) – ASPECTO project (grant 88887.091731/2014–01) and the Fundação de Amparo à Pesquisa do Estado de São Paulo (FAPESP) project (grant 2022/03830-3). M.O. Tomazella gratefully acknowledges the CAPES scholarship (grant 88887.388307/2019-00). We also would like to thank the reviewers for their insightful suggestions.

AUTHOR CONTRIBUTIONS

M.O.T.: Conceptualization; Investigation; Methodology; Formal Analysis; Writing – original draft; Writing – review & editing.

G.A.P., J.P.Q.: Conceptualization, Investigation, Writing – review & editing.

F.A.L.T.: Supervision, Project administration, Writing – review & editing.

K.B.C.: Supervision, Project administration, Funding acquisition, Writing – review & editing.

REFERENCES

Arz, H. W., Pätzold, J. & Wefer, G. 1998. Correlated millennial-scale changes in surface hydrography and terrigenous sediment yield inferred from last-glacial marine deposits off northeastern Brazil. *Quaternary*

Research, 50(2), 157-166. DOI: <https://doi.org/10.1006/qres.1998.1992>

Arz, H. W., Pätzold, J., & Wefer, G. 1999. The deglacial history of the western tropical Atlantic as inferred from high resolution stable isotope records off northeastern Brazil. *Earth and Planetary Science Letters*, 167(1-2), 105-117. DOI: [https://doi.org/10.1016/s0012-821x\(99\)00025-4](https://doi.org/10.1016/s0012-821x(99)00025-4)

Arz, H. W., Gerhardt, S., Pätzold, J. & Röhl, U. 2001. Millennial-scale changes of surface- and deep-water flow in the western tropical Atlantic linked to northern hemisphere high-latitude climate during the Holocene. *Geology*, 29(3), 239. DOI: [https://doi.org/10.1130/0091-7613\(2001\)029<0239:mscosa>2.0.co;2](https://doi.org/10.1130/0091-7613(2001)029<0239:mscosa>2.0.co;2)

Bachu, S. 2000. Sequestration of CO₂ in geological media: Criteria and approach for site selection in response to climate change. *Energy Conversion and Management*, 41(9), 953-970. DOI: [https://doi.org/10.1016/s0196-8904\(99\)00149-1](https://doi.org/10.1016/s0196-8904(99)00149-1)

Bainbridge, A. E. & Geosecs. 1981. Hydrographic measurements during the GEOSECS Atlantic expedition. *PANGAEA*. DOI: <https://doi.org/10.1594/PANGAEA.824122>

Balch, W. M., Drapeau, D. T. & Fritz, J. J. 2000. Monsoonal forcing of calcification in the Arabian Sea. *Deep Sea Research Part II: Topical Studies in Oceanography*, 47(7-8), 1301-1337. DOI: [https://doi.org/10.1016/s0967-0645\(99\)00145-9](https://doi.org/10.1016/s0967-0645(99)00145-9)

Baumann, K., Böckel, B. & Frenz, M. 2004. Coccolith contribution to south Atlantic carbonate sedimentation. *Coccolithophores*, 367-402. DOI: https://doi.org/10.1007/978-3-662-06278-4_14

Behling, H., W. Arz, H., Pätzold, J. & Wefer, G. 2000. Late Quaternary vegetational and climate dynamics in northeastern Brazil, inferences from marine core GeoB 3104-1. *Quaternary Science Reviews*, 19(10), 981-994. DOI: [https://doi.org/10.1016/s0277-3791\(99\)00046-3](https://doi.org/10.1016/s0277-3791(99)00046-3)

Berger, W. H. 1973. Deep-sea carbonates; Pleistocene dissolution cycles. *The Journal of Foraminiferal Research*, 3(4), 187-195. DOI: <https://doi.org/10.2113/gsjfr.3.4.187>

Berger, W. H., Bonneau, M. C. & Parker, F. L. 1982. Foraminifera on the deep-sea floor-lysocline and dissolution rate. *Oceanologica Acta*, 5(2), 249-258. Available from: <https://archimer.ifremer.fr/doc/00120/23161/>

Bischoff, W. D., Bishop, F. C. & Mackenzie, F. T. 1983. Biogenically produced magnesian calcite; inhomogeneities in chemical and physical properties; comparison with synthetic phases. *American Mineralogist*, 68(11-12), 1183-1188.

Blaauw, M. & Christen, J. A. 2011. Flexible paleoclimate age-depth models using an autoregressive gamma process. *Bayesian Analysis*, 6(3). DOI: <https://doi.org/10.1214/11-ba618>

Bordin, L. H., Machado, E. D., Carvalho, M., Freire, A. S. & Fonseca, A. L. 2019. Nutrient and carbon dynamics under the water mass seasonality on the continental shelf at the south Brazil bight. *Journal of Marine Systems*, 189, 22-35. DOI: <https://doi.org/10.1016/j.jmarsys.2018.09.006>

- Brandini, F. P., Tura, P. M. & Santos, P. P. 2018. Ecosystem responses to biogeochemical fronts in the south Brazil bight. *Progress in Oceanography*, 164, 52-62. DOI: <https://doi.org/10.1016/j.pocean.2018.04.012>
- Broecker, W. S., Turekian, K. K. & Heezen, B. C. 1958. The relation of deep sea [Atlantic Ocean] sedimentation rates to variations in climate. *American Journal of Science*, 256(7), 503-517. DOI: <https://doi.org/10.2475/ajs.256.7.503>
- Broecker, W. S. 1982. Glacial to interglacial changes in ocean chemistry. *Progress in Oceanography*, 11(2), 151-197. DOI: [https://doi.org/10.1016/0079-6611\(82\)90007-6](https://doi.org/10.1016/0079-6611(82)90007-6)
- Broecker, W. S. & Peng, T. 1986. Carbon cycle: 1985 glacial to interglacial changes in the operation of the global carbon cycle. *Radiocarbon*, 28(2A), 309-327. DOI: <https://doi.org/10.1017/s0033822200007414>
- Broecker, W. S. & Clark, E. 1999. CaCO₃ size distribution: A paleocarbonate ion proxy? *Paleoceanography*, 14(5), 596-604. DOI: <https://doi.org/10.1029/1999pa900016>
- Broecker, W. S. & Clark, E. 2001. Reevaluation of the CaCO₃ size index paleocarbonate ion proxy. *Paleoceanography*, 16(6), 669-671. DOI: <https://doi.org/10.1029/2001pa000660>
- Broecker, W. 2003. The oceanic CaCO₃ cycle. *Treatise on Geochemistry*, 529-549. DOI: <https://doi.org/10.1016/b0-08-043751-6/06119-3>
- Broecker, W. 2009. Wally's quest to understand the ocean's CaCO₃ cycle. *Annual Review of Marine Science*, 1(1), 1-18. DOI: <https://doi.org/10.1146/annurev.marine.010908.163936>
- Buitenhuis, E., Van Bleijswijk, J., Bakker, D. & Veldhuis, M. 1996. Trends in inorganic and organic carbon in a bloom of *Emiliania huxleyi* in the North Sea. *Marine Ecology Progress Series*, 143, 271-282. DOI: <https://doi.org/10.3354/meps143271>
- Campos, E. J., Gonçalves, J. E. & Ikeda, Y. 1995. Water mass characteristics and geostrophic circulation in the south Brazil bight: Summer of 1991. *Journal of Geophysical Research: Oceans*, 100(C9), 18537-18550. DOI: <https://doi.org/10.1029/95jc01724>
- Campos, E. J., Lentini, C. A., Miller, J. L. & Piola, A. R. 1999. Interannual variability of the sea surface temperature in the south Brazil bight. *Geophysical Research Letters*, 26(14), 2061-2064. DOI: <https://doi.org/10.1029/1999gl900297>
- Charles, C. D. & Fairbanks, R. G. 1990. Glacial to interglacial changes in the isotopic gradients of Southern Ocean surface water. *Geological History of the Polar Oceans: Arctic versus Antarctic*, 519-538. DOI: https://doi.org/10.1007/978-94-009-2029-3_30
- Chiu, T. & Broecker, W. S. 2008. Toward better paleocarbonate ion reconstructions: New insights regarding the CaCO₃ size index. *Paleoceanography*, 23(2). DOI: <https://doi.org/10.1029/2008pa001599>
- Ciotti, Á. M., Odebrecht, C., Fillmann, G. & Moller, O. O. 1995. Freshwater outflow and subtropical convergence influence on phytoplankton biomass on the southern Brazilian continental shelf. *Continental Shelf Research*, 15(14), 1737-1756. DOI: [https://doi.org/10.1016/0278-4343\(94\)00091-z](https://doi.org/10.1016/0278-4343(94)00091-z)
- Cirano, M., Mata, M. M., Campos, E. J. & Deiró, N. F. 2006. A circulação Oceânica de larga-escala na região oeste do Atlântico Sul com base no modelo de circulação global OCCAM. *Revista Brasileira de Geofísica*, 24(2), 209-230. DOI: <https://doi.org/10.1590/s0102-261x2006000200005>
- Clark, P. U., Pisias, N. G., Stocker, T. F. & Weaver, A. J. 2002. The role of the thermohaline circulation in abrupt climate change. *Nature*, 415(6874), 863-869. DOI: <https://doi.org/10.1038/415863a>
- Cronin, T. M., Demartino, D. M., Dwyer, G. S. & Rodriguez-Lazaro, J. (1999). Deep-sea ostracode species diversity: Response to late Quaternary climate change. *Marine Micropaleontology*, 37(3-4), 231-249. DOI: [https://doi.org/10.1016/s0377-8398\(99\)00026-2](https://doi.org/10.1016/s0377-8398(99)00026-2)
- Crowley, T. J. 1983. Calcium-carbonate preservation patterns in the central North Atlantic during the last 150,000 years. *Marine Geology*, 51(1-2), 1-14. DOI: [https://doi.org/10.1016/0025-3227\(83\)90085-3](https://doi.org/10.1016/0025-3227(83)90085-3)
- Curry, W. B. & Crowley, T. J. 1987. The $\delta^{13}\text{C}$ of equatorial Atlantic surface waters: Implications for ice age pCO₂ levels. *Paleoceanography*, 2(5), 489-517. DOI: <https://doi.org/10.1029/pa002i005p00489>
- Curry, W. B. & Oppo, D. W. 2005. Glacial water mass geometry and the distribution of $\delta^{13}\text{C}$ of ΣCO_2 in the western Atlantic Ocean. *Paleoceanography*, 20(1). DOI: <https://doi.org/10.1029/2004pa001021>
- De Mahiques, M. M., Tessler, M. G., Maria Ciotti, A., Da Silveira, I. C., E Sousa, S. H., Figueira, R. C., Tassinari, C. C., Furtado, V. V. & Passos, R. F. 2004. Hydrodynamically driven patterns of recent sedimentation in the shelf and upper slope off southeast Brazil. *Continental Shelf Research*, 24(15), 1685-1697. DOI: <https://doi.org/10.1016/j.csr.2004.05.013>
- De Mahiques, M. M., Coaracy Wainer, I. K., Burone, L., Nagai, R., De Mello E Sousa, S. H., Lopes Figueira, R. C., Almeida Da Silveira, I. C., Bicego, M. C., Vicente Alves, D. P. & Hammer, Ø. 2009. A high-resolution Holocene record on the southern Brazilian shelf: Paleoenvironmental implications. *Quaternary International*, 206(1-2), 52-61. DOI: <https://doi.org/10.1016/j.quaint.2008.09.010>
- Dittert, N., Baumann, K., Bickert, T., Henrich, R., Huber, R., Kinkel, H. & Meggers, H. 1999. Carbonate dissolution in the deep-sea: Methods, quantification and Paleoceanographic application. *Use of Proxies in Paleoceanography*, 255-284. DOI: https://doi.org/10.1007/978-3-642-58646-0_10
- Ducklow, H., Steinberg, D. & Buesseler, K. 2001. Upper ocean carbon export and the biological pump. *Oceanography*, 14(4), 50-58. DOI: <https://doi.org/10.5670/oceanog.2001.06>
- Dymond, J. & Collier, R. 1988. Biogenic particle fluxes in the equatorial Pacific: Evidence for both high and low productivity during the 1982-1983 El Niño. *Global Biogeochemical Cycles*, 2(2), 129-137. DOI: <https://doi.org/10.1029/gb002i002p00129>
- Emilsson, I. 1961. The shelf and coastal waters off southern Brazil. *Boletim do Instituto Oceanográfico*, 11(2), 101-112. DOI: <https://doi.org/10.1590/s0373-55241961000100004>

- Falkowski, P. G. 1997. Evolution of the nitrogen cycle and its influence on the biological sequestration of CO₂ in the ocean. *Nature*, 387(6630), 272-275. DOI: <https://doi.org/10.1038/387272a0>
- Farrell, J. W. & Prell, W. L. 1989. Climatic change and CaCO₃ preservation: An 800,000-year bathymetric reconstruction from the central equatorial Pacific Ocean. *Paleoceanography*, 4(4), 447-466. DOI: <https://doi.org/10.1029/pa004i004p00447>
- Feely, R. A., Sabine, C. L., Lee, K., Berelson, W., Kleypas, J., Fabry, V. J. & Millero, F. J. 2004. Impact of anthropogenic CO₂ on the CaCO₃ system in the oceans. *Science*, 305(5682), 362-366. DOI: <https://doi.org/10.1126/science.1097329>
- Figueiredo, T. S., Santos, T. P., Costa, K. B., Toledo, F., Albuquerque, A. L., Smoak, J. M., Bergquist, B. A. & Silva-Filho, E. V. 2020. Effect of deep southwestern subtropical Atlantic Ocean circulation on the biogeochemistry of mercury during the last two glacial/interglacial cycles. *Quaternary Science Reviews*, 239, 106368. DOI: <https://doi.org/10.1016/j.quascirev.2020.106368>
- Frenz, M., Baumann, K., Boeckel, B., Hoppner, R. & Henrich, R. 2005. Quantification of foraminifer and coccolith carbonate in south Atlantic surface sediments by means of carbonate grain-size distributions. *Journal of Sedimentary Research*, 75(3), 464-475. DOI: <https://doi.org/10.2110/jsr.2005.036>
- Frenz, M. & Henrich, R. 2006. Carbonate dissolution revealed by silt grain-size distribution: Comparison of Holocene and last glacial maximum sediments from the pelagic south Atlantic. *Sedimentology*, 54(2), 391-404. DOI: <https://doi.org/10.1111/j.1365-3091.2006.00841.x>
- Gaeta, S. A. & Brandini, F. P. 2006. Produção primária do fitoplâncton na região entre o Cabo de São Tomé (RJ) e o Chuí (RS). *O ambiente oceanográfico da plataforma continental e do talude na região sudeste-sul do Brasil, São Paulo, SP, Brasil, EDUSP*, 219-264.
- Gardner, J. V. 1975. Late Pleistocene carbonate dissolution cycles in the eastern equatorial Atlantic. In: Sliter, W. V., Bé, A. W. & Berger, W. H. *Dissolution of deep-sea carbonates* (pp. 129-141). Lawrence: Cushman Foundation for Foraminiferal Research Inc.
- Gonzales, M. V., de Almeida, F. K., Costa, K. B., Santarosa, A. C., Camillo, E., de Quadros, J. P. & Toledo, F. A. 2017. Help index: *Hoeglundina elegans* preservation index for marine sediments in the western south Atlantic. *The Journal of Foraminiferal Research*, 47(1), 56-69. DOI: <https://doi.org/10.2113/gsjfr.47.1.56>
- Govin, A., Holzwarth, U., Heslop, D., Ford Keeling, L., Zabel, M., Mülitz, S., Collins, J. A. & Chiessi, C. M. 2012. Distribution of major elements in Atlantic surface sediments (36°N–49°S): Imprint of terrigenous input and continental weathering. *Geochemistry, Geophysics, Geosystems*, 13(1). DOI: <https://doi.org/10.1029/2011gc003785>
- Govin, A., Chiessi, C. M., Zabel, M., Sawakuchi, A. O., Heslop, D., Hörner, T., Zhang, Y. & Mülitz, S. 2014. Terrigenous input off northern South America driven by changes in Amazonian climate and the north Brazil current retroflection during the last 250 Ka. *Climate of the Past*, 10(2), 843-862. DOI: <https://doi.org/10.5194/cp-10-843-2014>
- Gyllencreutz, R., Mahiques, M., Alves, D. & Wainer, I. 2010. Mid- to late-Holocene paleoceanographic changes on the southeastern Brazilian shelf based on grain size records. *The Holocene*, 20(6), 863-875. DOI: <https://doi.org/10.1177/0959683610365936>
- Hales, B. 2003. Respiration, dissolution, and the lysocline. *Paleoceanography*, 18(4). DOI: <https://doi.org/10.1029/2003pa000915>
- Hassenkam, T., Johnsson, A., Bechgaard, K. & Stipp, S. L. 2011. Tracking single coccolith dissolution with picogram resolution and implications for CO₂ sequestration and ocean acidification. *Proceedings of the National Academy of Sciences*, 108(21), 8571-8576. DOI: <https://doi.org/10.1073/pnas.1009447108>
- Hay, W. 1970. Calcareous Nannofossils from cores recovered on leg 4. *Initial Reports of the Deep Sea Drilling Project*. DOI: <https://doi.org/10.2973/dsdp.proc.4.123.1970>
- Hays, J. D. & Perruzza, A. 1972. The significance of calcium carbonate oscillations in eastern equatorial Atlantic deep-sea sediments for the end of the Holocene warm interval. *Quaternary Research*, 2(3), 355-362. DOI: [https://doi.org/10.1016/0033-5894\(72\)90058-0](https://doi.org/10.1016/0033-5894(72)90058-0)
- Honjo, S. 1975. Dissolution of suspended coccoliths in the deep-sea water column and sedimentation of coccolith ooze. In: Sliter, W. V., Bé, A. W., & Berger, W. H. (1975). *Dissolution of deep-sea carbonates*.
- Honjo, S. 1976. Coccoliths: Production, transportation and sedimentation. *Marine Micropaleontology*, 1, 65-79. DOI: [https://doi.org/10.1016/0377-8398\(76\)90005-0](https://doi.org/10.1016/0377-8398(76)90005-0)
- Honjo, S., Manganini, S. J. & Cole, J. J. 1982. Sedimentation of biogenic matter in the deep ocean. *Deep Sea Research Part A. Oceanographic Research Papers*, 29(5), 609-625. DOI: [https://doi.org/10.1016/0198-0149\(82\)90079-6](https://doi.org/10.1016/0198-0149(82)90079-6)
- Kullenberg, B. 1953. Absolute chronology of deep-sea sediments and the deposition of clay on the ocean floor. *Tellus*, 5(3), 302-305. DOI: <https://doi.org/10.1111/j.2153-3490.1953.tb01058.x>
- Lea, D. W., Martin, P. A., Pak, D. K. & Spero, H. J. 2002. Reconstructing a 350ky history of sea level using planktonic Mg/Ca and oxygen isotope records from a cocos ridge core. *Quaternary Science Reviews*, 21(1-3), 283-293. DOI: [https://doi.org/10.1016/s0277-3791\(01\)00081-6](https://doi.org/10.1016/s0277-3791(01)00081-6)
- Leite, Y. L., Costa, L. P., Loss, A. C., Rocha, R. G., Batalha-Filho, H., Bastos, A. C., Quaresma, V. S., Fagundes, V., Paresque, R., Passamani, M. & Pardini, R. 2016. Neotropical forest expansion during the last glacial period challenges refuge hypothesis. *Proceedings of the National Academy of Sciences*, 113(4), 1008-1013. DOI: <https://doi.org/10.1073/pnas.1513062113>
- Lessa, D. V., Santos, T. P., Venancio, I. M., Santarosa, A. C., Dos Santos Junior, E. C., Toledo, F. A., Costa, K. B. & Albuquerque, A. L. 2019. Eccentricity-induced expansions of Brazilian coastal upwelling zones. *Global and Planetary Change*, 179, 33-42. DOI: <https://doi.org/10.1016/j.gloplacha.2019.05.002>

- Lisiecki, L. E. & Raymo, M. E. 2005. A Pliocene-Pleistocene stack of 57 globally distributed benthic $\delta^{18}\text{O}$ records. *Paleoceanography*, 20(1). DOI: <https://doi.org/10.1029/2004pa001071>
- Mathias, G. L., Nagai, R. H., Trindade, R. I. & de Mahiques, M. M. 2014. Magnetic fingerprint of the late Holocene inception of the Rio de La Plata plume onto the southeast Brazilian shelf. *Palaeogeography, Palaeoclimatology, Palaeoecology*, 415, 183-196. DOI: <https://doi.org/10.1016/j.palaeo.2014.03.034>
- Mathias, G. L., Roud, S. C., Chiessi, C. M., Campos, M. C., Dias, B. B., Santos, T. P., Albuquerque, A. L., Toledo, F. A., Costa, K. B. & Maher, B. A. 2021. A multi-proxy approach to unravel late Pleistocene sediment flux and bottom water conditions in the western south Atlantic Ocean. *Paleoceanography and Paleoclimatology*, 36(4). DOI: <https://doi.org/10.1029/2020pa004058>
- Millero, F. J. 1996. *Chemical oceanography* (2nd ed.). London: CRC Press.
- Milliman, J. D. 1993. Production and accumulation of calcium carbonate in the ocean: Budget of a nonsteady state. *Global Biogeochemical Cycles*, 7(4), 927-957. DOI: <https://doi.org/10.1029/93gb02524>
- Nagai, R. H., Sousa, S. H., Lourenço, R. A., Bicego, M. C. & Mahiques, M. M. 2010. Paleoproductivity changes during the late Quaternary in the southeastern Brazilian upper continental margin of the southwestern Atlantic. *Brazilian Journal of Oceanography*, 58(spe1), 31-41. DOI: <https://doi.org/10.1590/s1679-87592010000500004>
- Naik, S. S., Godad, S. P., Naidu, P. D., Tiwari, M. & Paropkari, A. L. 2014. Early- to late-Holocene contrast in productivity, OMZ intensity and calcite dissolution in the eastern Arabian Sea. *The Holocene*, 24(6), 749-755. DOI: <https://doi.org/10.1177/0959683614526936>
- Olausson, E. 1965. Climatological, geoeconomical and paleoceanographical aspects on carbonate deposition. *Progress in Oceanography*, 4, 245-265. DOI: [https://doi.org/10.1016/0079-6611\(65\)90053-4](https://doi.org/10.1016/0079-6611(65)90053-4)
- Olausson, E. 1971, June. 29. QUATERNARY CORRELATIONS AND THE GEOCHEMISTRY OF OZES. In: *The Micropalaeontology of Oceans: Proceedings of the Symposium Held in Cambridge from 10 to 17 September 1967 Under the Title 'Micropalaeontology of Marine Bottom Sediments'* (p. 375). Cambridge: Cambridge University Press.
- Pedrao, G. A., Costa, K. B., Toledo, F. A., Tomazella, M. O. & Jovane, L. 2021. Semi-quantitative analysis of major elements and minerals: Clues from a late Pleistocene core from campos basin. *Applied Sciences*, 11(13), 6206. DOI: <https://doi.org/10.3390/app11136206>
- Pedrao, G. A., Hiram, M. V., Tomazella, M. O., Albuquerque, A. L., Chiessi, C. M., Costa, K. B. & Toledo, F. A. 2022. Marine Paleoproductivity from the last glacial maximum to the Holocene in the southwestern Atlantic: A Coccolithophore assemblage and geochemical proxy perspective. *Frontiers in Earth Science*, 10. DOI: <https://doi.org/10.3389/feart.2022.846245>
- Pereira, L. S., Arz, H. W., Pätzold, J. & Portilho-Ramos, R. C. 2018. Productivity evolution in the south Brazilian bight during the last 40,000 years. *Paleoceanography and Paleoclimatology*, 33(12), 1339-1356. DOI: <https://doi.org/10.1029/2018pa003406>
- Peterson, R. G. & Stramma, L. 1991. Upper-level circulation in the south Atlantic Ocean. *Progress in Oceanography*, 26(1), 1-73. DOI: [https://doi.org/10.1016/0079-6611\(91\)90006-8](https://doi.org/10.1016/0079-6611(91)90006-8)
- Petró, S. M. & Burone, L. 2018. Changes in water masses in the late Quaternary recorded at Uruguayan continental slope (South Atlantic Ocean) / Mudanças nas massas de água durante o Quaternário tardio registradas no talude continental Uruguaio (Oceano Atlântico Sul). *Journal of Sedimentary Environments*, 3(4), 280-289. DOI: <https://doi.org/10.12957/jse.2018.39156>
- Petró, S. M., Costa, E. O., Pivel, M. A. & Coimbra, J. C. 2018. Lysocline and CCD fluctuations record in pelotas basin during the late Quaternary. *Anuário do Instituto de Geociências - UFRJ*, 41(2), 710-719. DOI: https://doi.org/10.11137/2018_2_710_719
- Petró, S. M., Pivel, M. A. & Coimbra, J. C. 2021. Evidence of supra-lysocline dissolution of pelagic calcium carbonate in the late Quaternary in the western south Atlantic. *Marine Micropaleontology*, 166, 102013. DOI: <https://doi.org/10.1016/j.marmicro.2021.102013>
- Piola, A. R., Campos, E. J., Möller, O. O., Charo, M. & Martinez, C. 2000. Subtropical shelf front off eastern South America. *Journal of Geophysical Research: Oceans*, 105(C3), 6565-6578. DOI: <https://doi.org/10.1029/1999jc000300>
- Pivel, M., Santarosa, A., Toledo, F. & Costa, K. 2013. The Holocene onset in the southwestern south Atlantic. *Palaeogeography, Palaeoclimatology, Palaeoecology*, 374, 164-172. DOI: <https://doi.org/10.1016/j.palaeo.2013.01.014>
- Pogge Von Strandmann, P. A., Forshaw, J. & Schmidt, D. N. 2014. Modern and Cenozoic records of seawater magnesium from foraminiferal mg isotopes. *Biogeosciences*, 11(18), 5155-5168. DOI: <https://doi.org/10.5194/bg-11-5155-2014>
- Portilho-Ramos, R. D., Pinho, T. M., Chiessi, C. M. & Barbosa, C. F. 2019. Understanding the mechanisms behind high glacial productivity in the southern Brazilian margin. *Climate of the Past*, 15(3), 943-955. DOI: <https://doi.org/10.5194/cp-15-943-2019>
- Rahmstorf, S. 2002. Ocean circulation and climate during the past 120,000 years. *Nature*, 419(6903), 207-214. DOI: <https://doi.org/10.1038/nature01090>
- Ramaswamy, V. & Gaye, B. 2006. Regional variations in the fluxes of foraminifera carbonate, coccolithophorid carbonate and biogenic opal in the northern Indian Ocean. *Deep Sea Research Part I: Oceanographic Research Papers*, 53(2), 271-293. DOI: <https://doi.org/10.1016/j.dsr.2005.11.003>
- Rühlemann, C., Müller, P. J. & Schneider, R. R. 1999. Organic carbon and carbonate as Paleoproductivity proxies: Examples from high and low productivity areas of the tropical Atlantic. *Use of Proxies in Paleoceanography*, 315-344. DOI: https://doi.org/10.1007/978-3-642-58646-0_12
- Santos, T. P., Lessa, D. O., Venancio, I. M., Chiessi, C. M., Multiza, S., Kuhnert, H., Govin, A., Machado, T., Costa, K. B., Toledo, F., Dias, B. B. & Albuquerque, A. L.

2017. Prolonged warming of the Brazil current precedes deglaciations. *Earth and Planetary Science Letters*, 463, 1-12. DOI: <https://doi.org/10.1016/j.epsl.2017.01.014>
- Santos, T. P., Ballalai, J. M., Franco, D. R., Oliveira, R. R., Lessa, D. O., Venancio, I. M., Chiessi, C. M., Kuhnert, H., Johnstone, H. & Albuquerque, A. L. 2020. Asymmetric response of the subtropical western south Atlantic thermocline to the Dansgaard-Oeschger events of marine isotope stages 5 and 3. *Quaternary Science Reviews*, 237, 106307. DOI: <https://doi.org/10.1016/j.quascirev.2020.106307>
- Schiebel, R. 2002. Planktic foraminiferal sedimentation and the marine calcite budget. *Global Biogeochemical Cycles*, 16(4). DOI: <https://doi.org/10.1029/2001gb001459>
- Schmiedl, G. & Mackensen, A. 1997. Late Quaternary paleoproductivity and deep water circulation in the eastern south Atlantic Ocean: Evidence from benthic foraminifera. *Palaeogeography, Palaeoclimatology, Palaeoecology*, 130(1-4), 43-80. DOI: [https://doi.org/10.1016/s0031-0182\(96\)00137-x](https://doi.org/10.1016/s0031-0182(96)00137-x)
- Schott, W. 1935. Die Sedimente des äquatorialen Atlantischen Ozeans. I. *Lieferung B. Die Foraminiferen in dem äquatorialen Teil des Atlantischen Ozeans. Deutsche-Atlantische Expedition*, 11(6), 43-134.
- Shackleton, N. J., Hall, M. A., Line, J. & Shuxi, C. 1983. Carbon isotope data in core V19-30 confirm reduced carbon dioxide concentration in the ice age atmosphere. *Nature*, 306(5941), 319-322. DOI: <https://doi.org/10.1038/306319a0>
- Silveira, I. C., Schmidt, A. C., Campos, E. J., Godoi, S. S. & Ikeda, Y. 2000. A Corrente do Brasil AO Largo Da costa leste brasileira. *Revista Brasileira de Oceanografia*, 48(2), 171-183. DOI: <https://doi.org/10.1590/s1413-7739200000200008>
- Stein, R. 1991. *Accumulation of organic carbon in marine sediments: Results from the Deep Sea Drilling Project/Ocean drilling program (DSDP/ODP)*. Berlin: Springer.
- Suárez-Ibarra, J. Y., Frozza, C. F., Palhano, P. L., Petró, S. M., Weinkauf, M. F. & Pivel, M. A. 2022. Calcium carbonate dissolution triggered by high productivity during the last glacial-interglacial interval in the deep western south Atlantic. *Frontiers in Earth Science*, 10. DOI: <https://doi.org/10.3389/feart.2022.830984>
- Thompson, P. R. & Saito, T. 1974. Pacific Pleistocene sediments: Planktonic foraminifera dissolution cycles and geochronology. *Geology*, 2(7), 333. DOI: [https://doi.org/10.1130/0091-7613\(1974\)2<333:ppspfd>2.0.co;2](https://doi.org/10.1130/0091-7613(1974)2<333:ppspfd>2.0.co;2)
- Thunell, R. C. 1976. Calcium carbonate dissolution history in late Quaternary deep-sea sediments, western Gulf of Mexico. *Quaternary Research*, 6(2), 281-297. DOI: [https://doi.org/10.1016/0033-5894\(76\)90055-7](https://doi.org/10.1016/0033-5894(76)90055-7)
- Toledo, F. A., Costa, K. B. & Pivel, M. A. 2007. Salinity changes in the western tropical south Atlantic during the last 30 kyr. *Global and Planetary Change*, 57(3-4), 383-395. DOI: <https://doi.org/10.1016/j.gloplacha.2007.01.001>
- Veres, D., Bazin, L., Landais, A., Toyé Mahamadou Kele, H., Lemieux-Dudon, B., Parrenin, F., Martinerie, P., Blayo, E., Blunier, T., Capron, E., Chappellaz, J., Rasmussen, S. O., Severi, M., Svensson, A., Vinther, B. & Wolff, E. W. (2013). The Antarctic ice core chronology (AICC2012): An optimized multi-parameter and multi-site dating approach for the last 120 thousand years. *Climate of the Past*, 9(4), 1733-1748. DOI: <https://doi.org/10.5194/cp-9-1733-2013>
- Volat, J., Pastouret, L. & Vergnaud-Grazzini, C. 1980. Dissolution and carbonate fluctuations in Pleistocene deep-sea cores: A review. *Marine Geology*, 34(1-2), 1-28. DOI: [https://doi.org/10.1016/0025-3227\(80\)90138-3](https://doi.org/10.1016/0025-3227(80)90138-3)
- Volk, T. & Hoffert, M. I. 1985. Ocean carbon pumps: Analysis of relative strengths and efficiencies in ocean-driven atmospheric CO₂ changes. *The Carbon Cycle and Atmospheric CO₂: Natural Variations Archaean to Present*, 99-110. DOI: <https://doi.org/10.1029/gm032p0099>
- Westbroek, P., Brown, C. W., Bleijswijk, J. V., Brownlee, C., Brummer, G. J., Conte, M., Egge, J., Fernández, E., Jordan, R., Knappertsbusch, M., Stefels, J., Veldhuis, M., Van Der Wal, P. & Young, J. 1993. A model system approach to biological climate forcing. The example of *Emiliania huxleyi*. *Global and Planetary Change*, 8(1-2), 27-46. DOI: [https://doi.org/10.1016/0921-8181\(93\)90061-r](https://doi.org/10.1016/0921-8181(93)90061-r)
- Zamelczyk, K., Rasmussen, T. L., Husum, K., Hafliðason, H., De Vernal, A., Ravna, E. K., Hald, M. & Hillaire-Marcel, C. 2012. Paleooceanographic changes and calcium carbonate dissolution in the central Fram strait during the last 20 Ka. *Quaternary Research*, 78(3), 405-416. DOI: <https://doi.org/10.1016/j.yqres.2012.07.006>
- Ziveri, P., Broerse, A. T., Van Hinte, J. E., Westbroek, P. & Honjo, S. 2000. The fate of coccoliths at 48°N 21°W, northeastern Atlantic. *Deep Sea Research Part II: Topical Studies in Oceanography*, 47(9-11), 1853-1875. DOI: [https://doi.org/10.1016/s0967-0645\(00\)00009-6](https://doi.org/10.1016/s0967-0645(00)00009-6)